Catalysis Today 147S (2009) S10–S16

Contents lists available at ScienceDirect

Catalysis Today

journal homepage: www.elsevier.com/locate/cattod

Microreactors with Pt/zeolite catalytic films for the selective oxidation of CO in simulated reformer streams

V. Sebastian, S. Irusta, R. Mallada, J. Santamaría *

Department of Chemical and Environmental Engineering and Nanoscience Institute of Aragón, University of Zaragoza, Zaragoza, Spain

ARTICLE INFO

Article history:
Available online 4 August 2009

Keywords:
CO SELOX
Selective oxidation
Microreactor
ETS-10
Platinum
Faujasite

ABSTRACT

The selective oxidation (SELOX) of CO in the presence of H_2, CO_2 and H_2O has been carried out on stainless steel microreactors with 500 μm diameter microchannels. To this end, catalytic films consisting of Pt supported on zeolite Y (Pt-FAU) or ETS-10 (Pt-ETS10), were prepared by seeded hydrothermal synthesis on the surface of the reactor microchannels to give a uniform, mechanically stable catalytic coating on the channel surface. Activity tests were performed with feeds consisting of CO and H_2, plus CO_2 and/or H_2O. The best performance was obtained on microreactors coated with Pt-FAU catalytic films. When feeds representative of real reformate streams (containing CO_2 and H_2O) were fed to Pt-FAU coated reactors, the microreactor clearly outperformed the fixed bed reactor giving light-off temperatures that were lower by almost 50 °C.

1. Introduction

The selective oxidation of carbon monoxide (SELOX) is being intensely investigated as an alternative to reduce the content of CO in proton exchange membrane fuel cell (PEMFC) systems. This reduction is critical, especially for mobile applications, where the fuel cell operates downstream from a reformer, and the CO concentration must be reduced below 10 ppm to avoid poisoning of the Pt catalyst at the cell anode. An attractive alternative for this level of CO reduction is the selective oxidation (SELOX) reaction, of carbon monoxide over Pt-supported catalysts [1]. On the other hand, on account of characteristics such as high heat and mass transfer rates, intrinsic safety and easy scale up [2–4] microreactors seem to be ideally suited for this reaction when coupled to PEMFC systems in low to medium power output applications.

The SELOX reaction has in fact been carried out in microreactors using different catalysts, generally based on Pt, such as Pt–Rh/CeO_2/SiO_2 [5]; Pt-ZSM-5 [6]; Pt-Al_2O_3 [7,8], or on Cu-ceria, such as Cu/CeO_2-x [9]; CuO/CeO_2 [10] deposited on the microreactor channels. Whatever the catalyst used, one of the main problems in the development of microreactors is the need to obtain a catalytic load that is: (i) reproducible, (ii) homogeneously distributed along the microreactor channels, (iii) mechanically stable, and (iv) sufficient to achieve the desired yield under a given set of reaction conditions. From the work of Meille [11] reviewing the available catalyst deposition methods it can be concluded that a universal method that satisfies the above requirements does not exist. In previous works in our laboratory [6,12] and in others [13–15]; the method chosen has been the growth of zeolite layers directly on the microchannel walls by means of hydrothermal synthesis. This provides a homogeneous, mechanically resistant coating with the added advantage of not requiring a secondary support or even a binder.

In this work the SELOX reaction has been carried out using microreactors whose walls had been coated with Pt-FAU and Pt-ETS10 films. In many of the above quoted investigations of the SELOX reaction in microreactors the process was carried out with feeds containing only H_2, CO and oxygen. While these are the main reactants, it is well established that the behaviour of Pt catalysts on different supports can vary considerably in the presence of significant amounts CO_2 and H_2O [16,17]. Because of this, in this work the microreactors have been employed with feeds containing CO_2 and/or water. The results have been compared to those previously obtained in fixed bed catalytic reactors under the same operating conditions [18].

2. Experimental

2.1. Catalytic microchannel reactors

The microreactors were provided by the Institut für Mikrotechnik Mainz (IMM) and consisted of two 314SS Plates (50 mm × 10 mm × 2 mm), containing each with 14 semicircular microchannels in each plate (length = 25 mm, diame-

* Corresponding author.
E-mail address: Jesus.Santamaria@unizar.es (J. Santamaría).

0920-5861/$ – see front matter © 2009 Elsevier B.V. All rights reserved.
doi:10.1016/j.cattod.2009.07.061

Table 1
Synthesis conditions: composition of the synthesis solutions, temperature and synthesis time for the different microporous supports prepared.

Material	Molar composition	Temperature (°C)	Time (h)
Zeolite Y Si/Al = 8	$Na_2O:SiO_2:Al_2O_3:H_2O$ 17:12.8:1:975	90	24
ETS-10 Si/Ti = 5	$Na_2O:SiO_2:TiO_2:K_2O:H_2O$ 3:5.6:1:1.8:280	200	72

ter = 500 μm). The synthesis of zeolite Y and ETS-10 layers over these microreactor plates was optimized in a previous work [12] to obtain a homogeneous, well adhered and accessible zeolite layer. Seeded hydrothermal synthesis was used, with the synthesis gel composition and operating conditions summarized in Table 1. In the case of zeolite Y, two successive hydrothermal syntheses were carried out, further details can be found elsewhere [12].

Pt was ion exchanged onto the zeolite films coating the microchannels by immersion into a stirred $[Pt(NH_3)_4](NO_3)_2$ solution during 24 h at 298 K (zeolite Y) or 333 K (ETS-10). After ion exchange the plates were thoroughly washed with distilled water and dried at 75 °C overnight. The subsequent reduction treatment often has a strong influence on Pt dispersion; in this work the conditions were selected based on the results of Graaf et al. [19] and consisted of heating to 350 °C under air at 0.2 °C/min, then calcination in air for 3 h at 350 °C, followed by reduction at this temperature under 10% H_2 in N_2 for 3 h, then cooling down in N_2. After synthesis and impregnation of the catalyst films, the two plates were joined together by a special TIG welding procedure (done at IMM) designed to avoid damage to the catalyst.

2.2. Characterization

The morphology and continuity of the zeolite films were examined by Scanning Electron Microscopy, SEM (JEOL JSM 6460 LV and HITACHI S2300), before and after reaction. To this end, after reaction the microreactors were opened, and some sections were cut and embedded in resin to obtain cross-section views of the microchannels. Energy Dispersive X-ray analysis (EDX) was performed in the zeolite layers, to determine the Pt content. In the case of zeolite Y, after synthesis and ion exchange, samples of the zeolite layer were detached from the support plate and analyzed by Inductive Coupled Plasma, ICP (PerkinElmer P-40). The crystallinity, purity and structure of the catalytic films were studied by X-ray Diffraction, XRD (Rygaku/Max System RU 300), before and after ion exchange. Thermogravimetric analyses (Mettler Toledo TGA/SDTA 851e equipment) were performed with zeolite Y and ETS-10 powders.

2.3. Activity tests

Two reactor feedstreams were used, namely reformate 1, with added CO_2 (1.25% CO, 26.01% CO_2, balance H_2) and reformate 2, with added CO_2 and H_2O (2.9% H_2O, 1.21% CO, 25.25% CO_2, balance H_2). The required oxygen concentration was added according to the λ value selected, with λ giving the oxygen excess vs. the stoichiometric amount required to oxidise all the CO in the feed, i.e., at λ = 1 the molar feed rate of oxygen would be 50% of the molar feed rate of CO. The weight hourly space velocity (WHSV) was 12,000 ml min^{-1} mg^{-1}.

An electrical furnace with a PID controller (Eurotherm 2216L) was used to heat the microreactors. Two thermocouples separated by 2 cm were placed in contact with the outer surface of the reactor along its axis, and the thermocouple near the exit was used to control the reactor temperature. The temperature difference between both thermocouples was lower than 1 °C. Gas compositions were analyzed by an on-line gas chromatograph (Varian MicroGC-4900) equipped with thermal conductivity detectors and two columns, CP740148 MS5A and CP740150 PPQ, for the analysis of permanent gases (H_2, O_2 and CO) and H_2O and CO_2, respectively. CH_4 formation was not observed during the experiments carried out in this work. The conversion of oxygen and the selectivity for the SELOX reaction were calculated according to the following expressions, where F_i corresponds to the molar flux of the corresponding species

$$\text{CO conversion } (\%) = \frac{F_{CO}^{Feed} - F_{CO}^{Outlet}}{F_{CO}^{Feed}} \times 100 \quad (1)$$

$$O_2 \text{ conversion } (\%) = \frac{F_{O_2}^{Feed} - F_{O_2}^{Outlet}}{F_{O_2}^{Feed}} \times 100 \quad (2)$$

$$\text{Selectivity } (\%) = 0.5 \times \frac{F_{CO}^{Feed} - F_{CO}^{Outlet}}{F_{O_2}^{Feed} - F_{O_2}^{Outlet}} \times 100 \quad (3)$$

Finally the T_{100} and T_{50} (or light-off temperature) values reported below indicate the temperatures at which the 100% and 50% CO conversion were reached, respectively. The comparison of the catalytic performance in microreactors and conventional fixed bed reactors for a given catalyst was carried out at the same space time and temperature.

3. Results

3.1. Characterization of the zeolite films

Duplicate samples of each of the zeolite coatings were prepared on microreactor plates and analysed for weight gain and Pt content following hydrothermal synthesis and ion exchange. The results are given in Table 2, together with the Pt content of powdered catalyst samples prepared under the same impregnation conditions. There is good reproducibility of the weight gain in all cases, in agreement with our previous works on seeded hydrothermal synthesis of zeolite films on microchannels [12]. Also, the Pt content is similar on both powder and film Pt/zeolite Y analysed by ICP (5.6 wt.% vs. 6.4 wt.%). EDX analyses show larger concentrations of Pt compared to ICP results (9–10% vs. 6–7%), which reflects accumulation of Pt in the outer regions of the zeolite film, a consequence of the impregnation process.

The SEM images in Fig. 1, show different top views of microchannels coated with Pt-ZY and Pt-ETS10 as prepared and also after more than 300 h of reaction. As can be observed, the morphology of the layer remains unchanged after use. The zeolite Y crystals, Fig. 1a–d retain its typical octahedral geometry [20] and the film present a good degree of crystal intergrowth. However, some 1–3 μm wide cracks are clearly visible, running across the film. In a previous work [12] it was shown that these cracks were a consequence of the drying process following hydrothermal synthesis and their dimension could be controlled by adjusting the temperature and duration of drying. In the case of ETS-10,

Table 2
Some characteristics of the microreactors prepared (MRFAU: microreactor coated with Pt-FAU films; MRETS10: microreactor coated with ETS-10 films).

Microreactor	Total weight gain (mg)	Weight gain/area (mg/cm²)	wt.% Pt (EDX)	wt.% Pt (ICP)	wt.% Pt in powder catalysts (ICP)
MRFAU_1	33.2	1.36	9.5	5.64	6.4
MRFAU_2	33.3	1.37	NA		
MRETS10_1	14.1	0.58	10.2	–	7.3
MRETS10_2	14.0	0.57	NA		

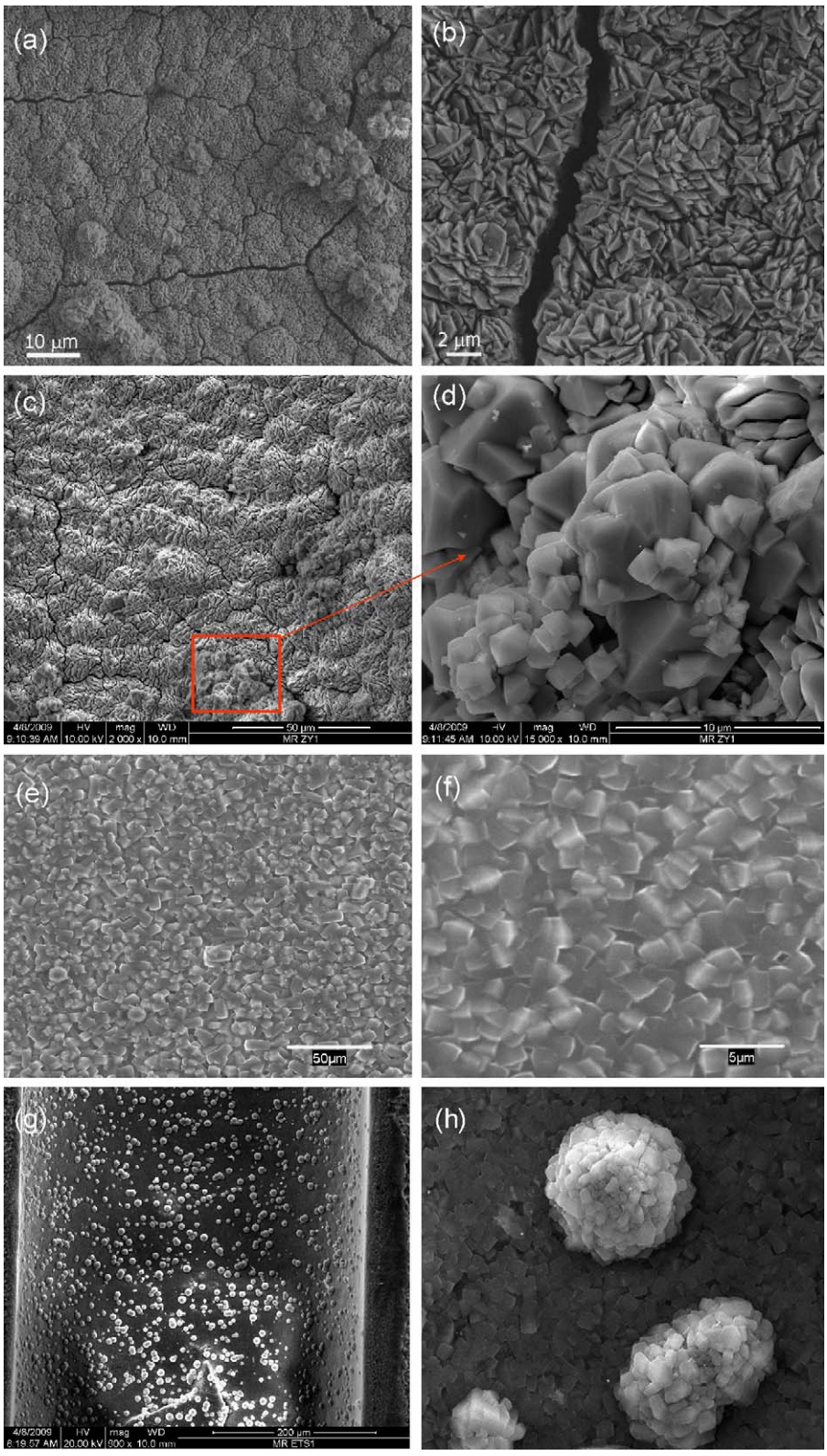

Fig. 1. (a and b) MRFAU before reaction, (c and d) MRFAU after reaction, (e and f) MRETS10 before reaction, and (g and h) MRETS10 after reaction.

although the morphology of the individual crystals is still the same after use (a detailed view is given in Fig. 1h), the texture of the surface has changed, with the emergence of hemispherical outgrowths with a size around 10 μm, a likely consequence of recrystallization processes during reaction.

The cross-section views (backscattered electron images) of the zeolite-coated microchannels, in Figs. 2a and 3a for ETS-10 and zeolite Y, respectively indicate a homogeneous distribution of the zeolite layer inside the channels, following the cylindrical surface of the channel. Fig. 2b is a SEM view of the ETS-10 layer, with a

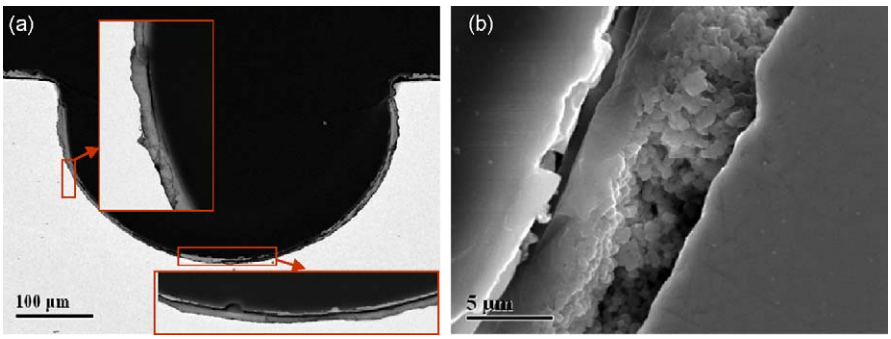

Fig. 2. SEM micrograph cross-section view, MRETS10_1. (a) Complete channel and (b) morphology details of the zeolite crystals in the layer.

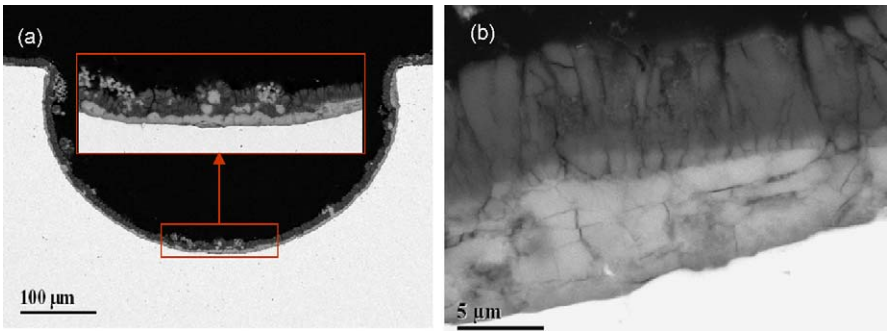

Fig. 3. SEM micrograph, cross-section view. (a) Complete channel and detail and (b) morphology of the zeolite crystals in the layer.

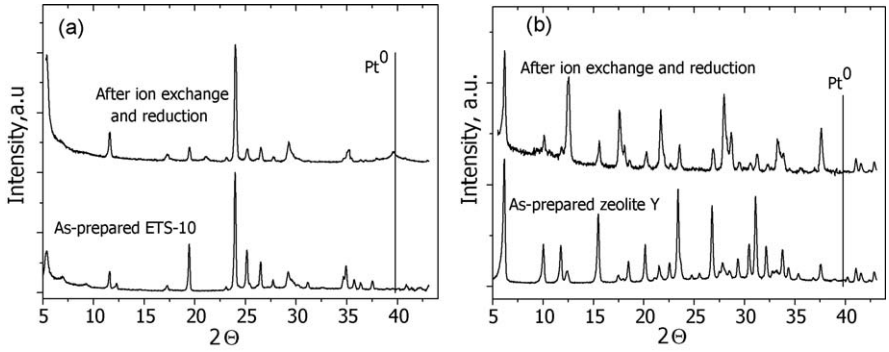

Fig. 4. XRD patterns of zeolite films grown on microreactor channels.

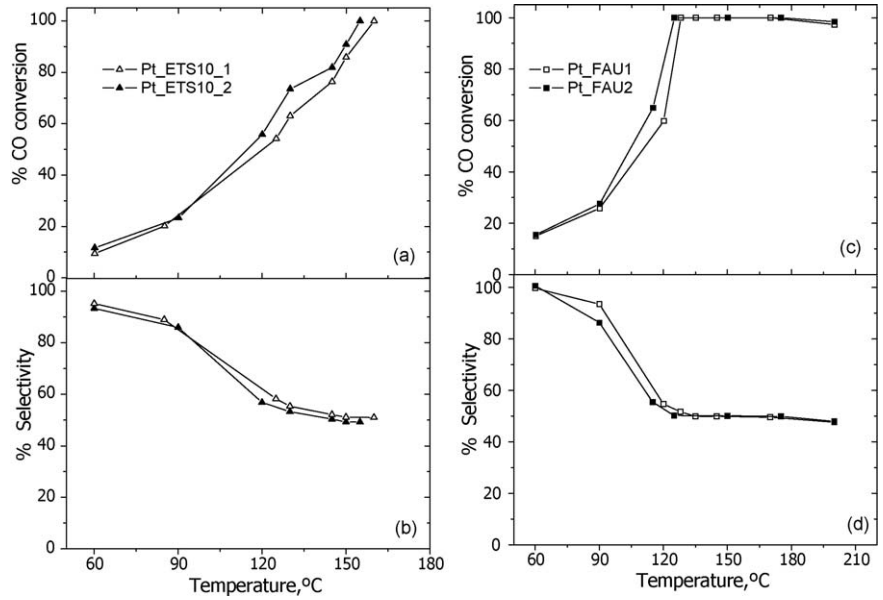

Fig. 5. Reproducibility of reactor performance for zeolite-coated reactors. (a and b) Conversion and selectivity for MRETS10_1 and MRETS10_2. Feed composition: 70.64% H_2, 2.9% H_2O, 1.21% CO, 25.25% CO_2; $\lambda = 2$, WHSV = 120,000 ml/h g. (c and d) Conversion and selectivity for MRFAU_1 and MRFAU_2.

thickness around 7.5 μm, where the constituting cubic crystals can be observed in detail. The thickness of the zeolite Y layer (SEM view in Fig. 3b) is larger, 10–15 μm, as a consequence of the two hydrothermal syntheses carried out. The two successive zeolite layers resulting from each synthesis are easily distinguished in Fig. 3b. In spite of the already mentioned cracks formed during drying, the zeolite Y layer is well adhered to the surface, and is able to resist a harsh treatment: after ultrasonication for 5 min, 93% of the crystals still remained in place.

X-ray diffraction patterns of the zeolite-coated channels, as prepared and after ion exchange and reduction are shown in Fig. 4. In both cases, the only zeolite phases present are well crystallized ETS-10 and FAU, respectively. In case of ETS-10 the reflexion of Pt° can be observed after ion exchange at $\theta = 37.1^{\circ}$, indicating the existence of Pt aggregates outside the microporous structure. This was also found in our previous work with a powdered Pt-ETS-10 catalyst with a similar Pt load [18]. The crystal size estimated from the Scherrer equation for these aggregates is 9 nm.

3.2. Reaction studies. I. Reproducibility of the preparation procedures for zeolite films

Although the comparison of SEM observations of duplicate samples of zeolite-coated microreactors (not shown) and the weight gain data in Table 2 seemed to indicate a good reproducibility of the preparation procedures, the best reproducibility test consists in comparing the reaction performance of different reactors. This is more demanding because by comparing reaction results we include not only the growth of the zeolite film on the microreactor channels, but also the repeatability of the Pt impregnation procedures and of the subsequent reduction treatments. In general, as the number of steps needed for the preparation of the catalyst increase, reproducibility becomes more difficult.

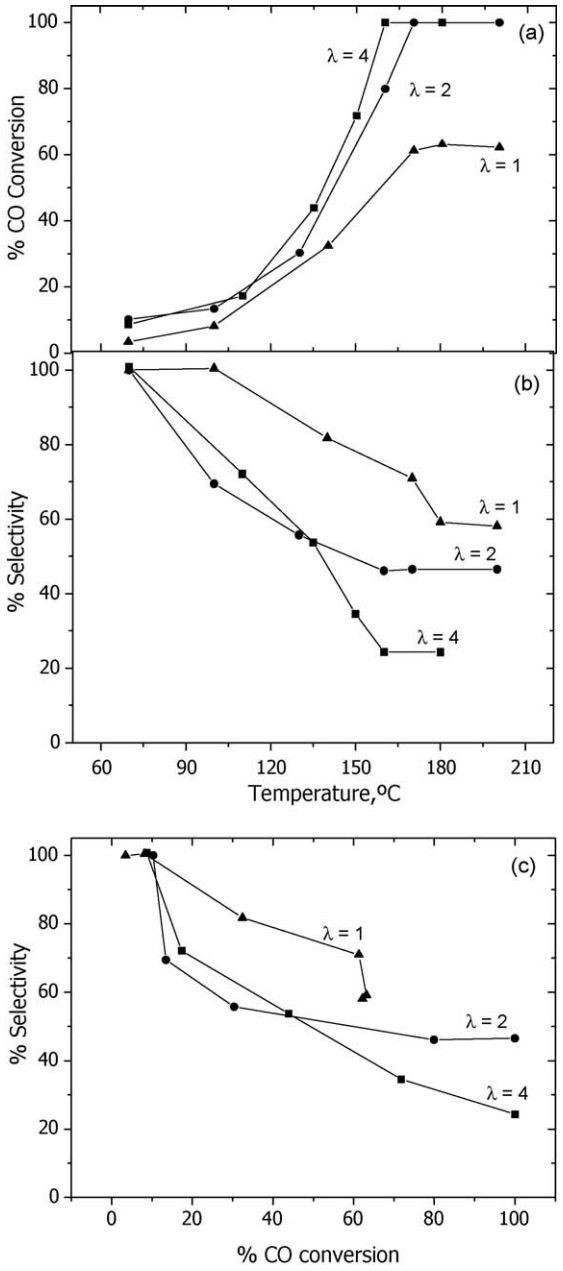

Fig. 6. Conversion (a) and selectivity (b) of the SELOX reaction on MRETS10_1 as a function of temperature, for different values of λ. Selectivity–conversion plot (c). Feed composition: 72.74% H_2, 1.25% CO, 26.01% CO_2; WHSV = 120,000 ml/h g.

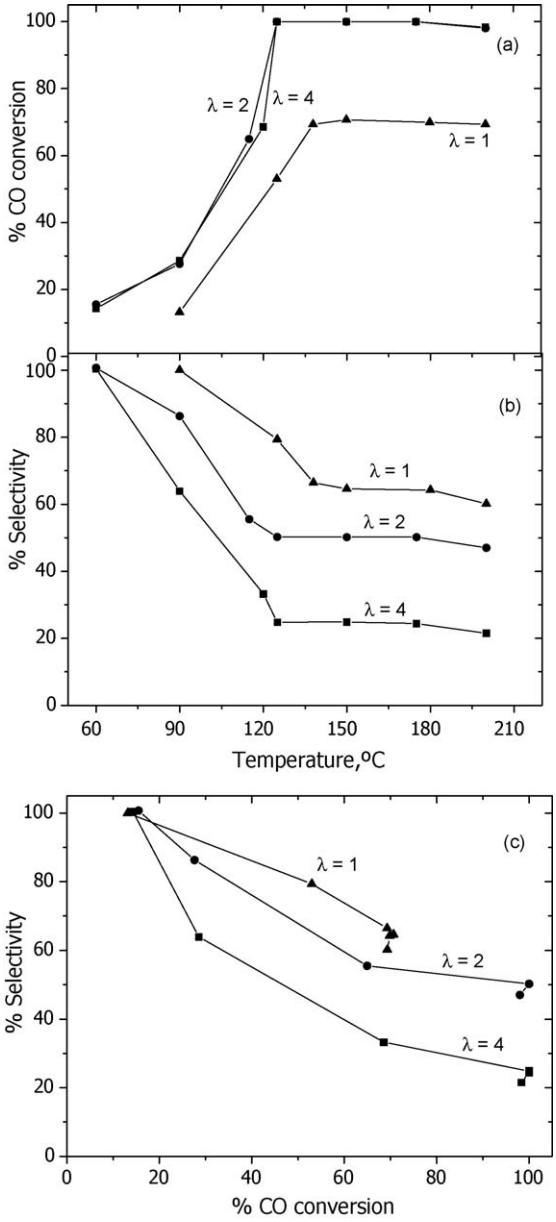

Fig. 7. Conversion (a) and selectivity (b) of the SELOX reaction on MRFAU_1 as a function of temperature, for different values of λ. Selectivity–conversion plot (c). Feed composition: 72.74% H_2, 1.25% CO, 26.01% CO_2; WHSV = 120,000 ml/h g.

Fig. 5 shows the variation of conversion and selectivity as a function of temperature for duplicate samples of the microreactors coated with Pt-ETS10 and Pt-FAU films. As can be observed, an excellent reproducibility was obtained for both types of catalytic microreactor: the light-off curves are reproduced within a temperature window smaller than 5 °C, and the selectivity also follows the same evolution with temperature for each of the duplicate samples.

3.3. Reaction studies. II. Microreactor performance

The conversion and selectivity obtained with microreactors MRETS10_1 and MRFAU_1 are presented in Figs. 6 and 7 as a function of temperature, for different λ values. As could be expected, since the reaction is not 100% selective, at stoichiometric concentrations there is not enough oxygen to convert all the CO in the feed, and total CO conversion was only reached at $\lambda \geq 2$, for both catalysts. Doubling the oxygen concentration from $\lambda = 2$ to $\lambda = 4$, did not result in a significant reduction of the T_{100} value, but decreased strongly the selectivity, especially at high conversions, as can be seen from the selectivity–conversion plot of Figs. 6c and 7c. For $\lambda = 2$ in the case of the ETS-10 microreactor, 100% conversion could be reached at $T_{100} = 170$ °C, while in the case of zeolite Y the T_{100} value was as low as 125 °C.

The influence of the feed composition, and in particular the beneficial effect of H_2O in the reactor feed is presented in Fig. 8 for both types of zeolite-coated microreactor. It can be seen that the addition of H_2O to a CO_2-containing feed has little effect for the Pt-FAU coated reactor (the light-off curve is shifted to lower temperatures by 5–10 °C), while a large improvement is observed for the microreactor coated with Pt-ETS10, where the shift is 20–30 °C. This follows the trends observed in the studies of the SELOX reactor with powdered catalysts in a fixed bed reactor [18] where an even larger shift was found for the Pt-ETS10 catalyst. This behaviour was explained [18] as a result of the dual effects of water on the catalyst surface: an increase of activity due to the formation of hydroxyl groups by the dissociative adsorption of H_2O on Pt, and an increase of the Bronsted acidity of the surface, reducing the basicity of the ETS-10 support and the inhibitory interaction of CO_2. In contrast, for microreactors coated with Pt-FAU catalytic films inhibition by CO_2 is not favoured in view of the acid nature of the support, and therefore the beneficial effect of water was limited.

The comparison of the performances of microreactors and fixed bed reactors for both types of catalyst is shown in Fig. 9 using the most realistic feed composition corresponding to reformate 2, i.e., containing H_2O and CO_2. As could be expected, the selectivity–conversion behaviour is not affected by the type of reactor, and for each type of catalyst the data corresponding to fixed bed reactor and microreactor roughly follow the same trend. However, significant differences can be observed when examining the evolution of conversion as a function of temperature. For the case of Pt-ETS10, both types of reactor give roughly the same performance, and the temperature for total conversion is only slightly lower for the microreactor. However, the lowest temperatures for total combustion were obtained for microreactors coated with Pt-FAU films (right hand side of Fig. 9). In this case the differences are considerable, and the light-off curve for the microreactor is shifted by 40–50 °C for most of the operating range. In view of these results, extended experiments were carried out using microreactors coated with Pt-FAU films, which showed stable performance (100% conversion and 50–52% selectivity) for 240 h on stream at 130 °C (results not shown).

The improvement obtained for the Pt-FAU catalyst can be explained as a consequence of the different diffusion lengths in both types of reactor. Although we attempted to use the smallest particle sizes available for operation in the fixed bed reactor, the particle size used in the reactor tests was in the 15–80 μm range meaning that the diffusion thickness for the fixed bed reactor is larger than for the microreactor. On the other hand, although the Pt-FAU film on the microreactor walls presented a thickness of 10–15 μm, the high degree of intergrowth in the film is expected to result in a compact layer of relatively high diffusion resistance. However, as seen in Fig. 1, this film is crossed by a network of cracks that penetrate the film and provide easy access of the reactants, reducing the diffusion lengths. This yields a catalytic film of high accessibility, with a low diffusion resistance that translates into lower reaction temperatures. For the case of the Pt-ETS10 films these cracks are not present, and the performance of the compact zeolite film is similar to that of the fixed bed reactor. It

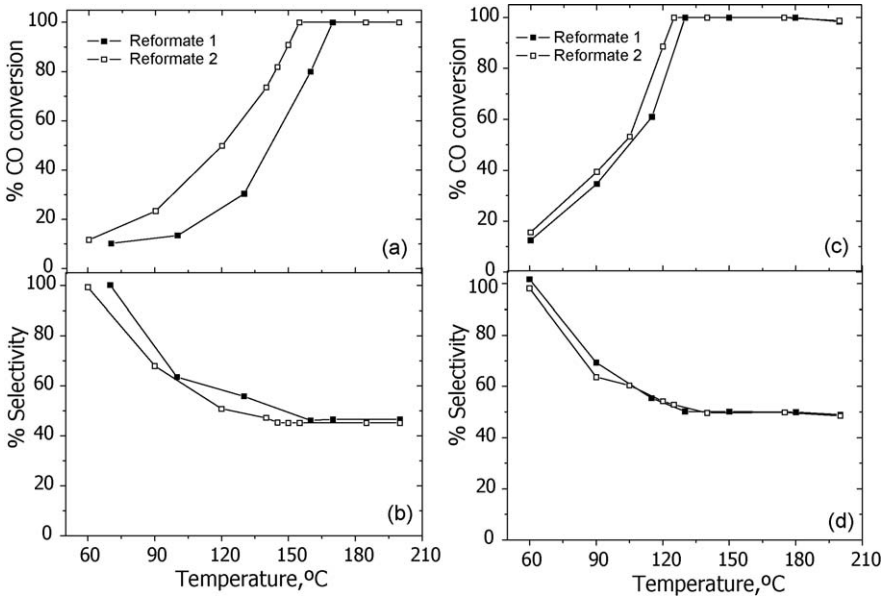

Fig. 8. Conversion and selectivity and of the SELOX reaction as a function of temperature for microreactors coated with Pt-ETS10 and Pt-FAU catalytic films and two different feed compositions. λ = 2, WHSV = 120,000 ml/h g. (a and b) MRETS10 and (c and d) MRFAU.

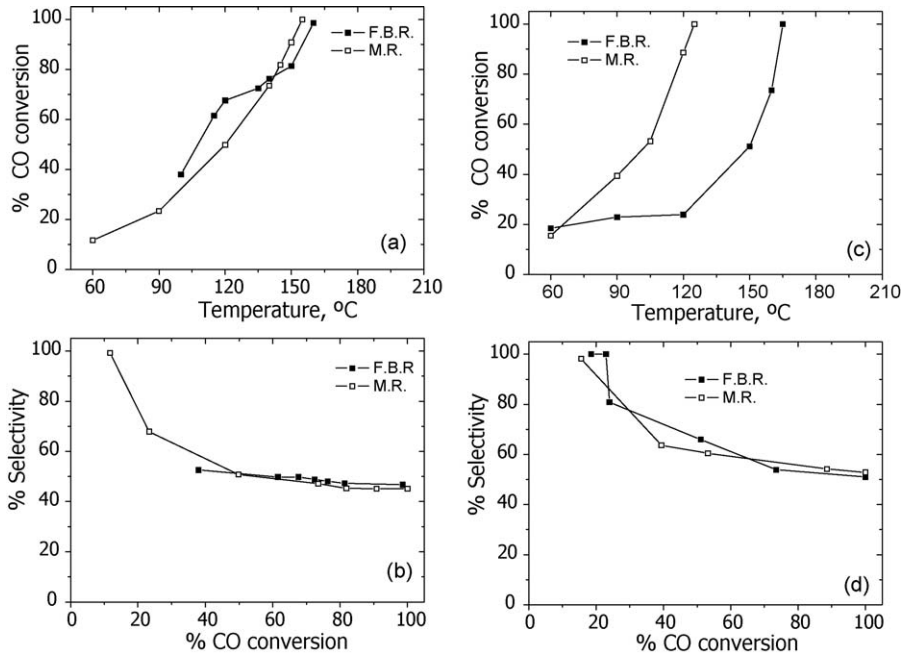

Fig. 9. Conversion and selectivity as a function of the temperature for MR vs. FBR. (a and b) ETS-10 and (c and d) FAU. Feed composition: 70.64% H_2, 2.9% H_2O, 1.21% CO, 25.25% CO_2; $\lambda = 2$, WHSV = 120,000 ml/h g.

must be taken into account, however, that in a real fixed bed reactor pressure drop constraints would lead to particle sizes in the mm range, and therefore of considerably larger size than those used here. In this case, the microreactor would provide a clear advantage, even for the compact Pt-ETS10 films. Alternatively, catalytic films can also be developed where the growth of individual crystals, rather than crystal intergrowth is the dominant feature, (see for instance [21] where this is carried out for mordenite coatings). Methods for producing this type of catalytic films for Pt-ETS10 are currently under investigation in our laboratory.

4. Conclusions

The SELOX reaction can be efficiently carried out on microreactors coated with Pt-ETS10 and Pt-FAU catalytic films. Seeded hydrothermal growth produced mechanically stable films with good catalytic performance. The best results were obtained for Pt-FAU films, in which the drying procedure resulted in the formation of cracks that provide faster diffusion avenues to the catalytic domains enclosed. With this catalyst, stable performance was obtained, with total CO combustion temperatures as low as 125 °C.

Acknowledgments

Financial support from MICINN, Spain, is gratefully acknowledged. One of the authors (SI) also acknowledges the receipt of a Ramon y Cajal grant.

References

[1] G. Kolb, V. Hessel, V. Cominos, C. Hofmann, H. Löwe, G. Nikolaidis, R. Zapf, A. Ziogas, E.R. Delsman, M.H.J.M. de Croon, J.C. Schouten, O. de la Iglesia, R. Mallada, J. Santamaria, Catal. Today 120 (2007) 2.
[2] K.F. Jensen, Chem. Eng. Sci. 56 (2001) 293.
[3] G. Kolb, V. Hessel, Chem. Eng. J. 98 (2004) 1.
[4] P.L. Mills, D. Quiram, J. Ryley, Chem. Eng. Sci. 62 (2007) 6992.
[5] G. Guan, R. Zapf, G. Kolb, V. Hessel, H. Lowe, J. Yec, R.R. Zentel, Int. J. Hydrogen Energy 33 (2008) 797.
[6] O. de la Iglesia, V. Sebastián, R. Mallada, G. Nikolaidis, J. Coronas, G. Kolb, R. Zapf, V. Hessel, J. Santamaría, Catal. Today 125 (2007) 2.
[7] X. Ouyang, R.S. Besser, J. Power Sources 141 (2005) 39.
[8] S.M. Hwang, O.J. Kwon, S.H. Ahn, J. Kim, Chem. Eng. J. 146 (2009) 105.
[9] P.V. Snytnikov, M.M. Popova, Y. Men, E.V. Rebrov, G. Kolb, V. Hessel, J.C. Schouten, V.A. Sobyanin, Appl. Catal. A: Gen. 350 (2008) 53.
[10] O. Goerke, P. Pfeifer, K. Schubert, Appl. Catal. A: Gen. 263 (2004) 11.
[11] V. Meille, Appl. Catal. A: Gen. 315 (2006) 1.
[12] V. Sebastián, O. de la Iglesia, R. Mallada, L. Casado, G. Kolb, V. Hessel, J. Santamaría, Microporous Mesoporous Mater. 115 (2008) 147.
[13] E.V. Rebrov, G.B. Seijger, H.P. Calis, M. de Croon, C.M. van den Bleek, J.C. Chouten, Appl. Catal. A: Gen. 206 (2001) 125.
[14] S.M. Lai, C.P. Ng, R. Martin-Aranda, K.L. Yeung, Microporous Mesoporous Mater. 66 (2003) 239.
[15] M.J.M. Mies, E.V. Rebrov, J.C. Jansen, M.H.M. de Croon, J.C. Schouten, J. Catal. 247 (2007) 328–338.
[16] J.L. Ayastuy, A. Gil-Rodriguez, M.P. Gonzáles-Marcos, M.A. Gutierrez-Ortiz, Int. J. Hydrogen Energy 31 (2006) 2231.
[17] A. Manasilp, E. Gulari, Appl. Catal. B Environ. 37 (2002) 17.
[18] V. Sebastian, S. Irusta, R. Mallada, J. Santamaría, Appl. Catal. A: Gen., in press, doi:10.1016/j.apcata.2009.06.044.
[19] J. Graaf, J. Pillen, K. Jong, D.C. Koningsberger, J. Catal. 203 (2001) 307.
[20] W. Lim, S. Choi, J. Choi, Y. Kim, N. Heo, K. Seff, Microporous Mesoporous Mater. 92 (2006) 234.
[21] M.A. Ulla, R. Mallada, L.B. Gutierrez, L. Casado, J.P. Bortolozzi, E.E. Miró, J. Santamaría, Catal. Today 133 (2008) 42–48.